

# Assembly of multiscale linear PDE operators

Miroslav Kuchta

**Abstract** In numerous applications the mathematical model consists of different processes coupled across a lower dimensional manifold. Due to the multiscale coupling, finite element discretization of such models presents a challenge. Assuming that only *singlescale* finite element forms can be assembled we present here a simple algorithm for representing multiscale models as linear operators suitable for Krylov methods. Flexibility of the approach is demonstrated by numerical examples with coupling across dimensionality gap 1 and 2. Preconditioners for several of the problems are discussed.

## 1 Introduction

This paper is concerned with implementation of the finite element method (FEM) for multiscale models, that is, systems where the unknowns are defined over domains of (in general) different topological dimension and are coupled on a manifold, which is possibly a different domain. The systems arise naturally in applications where Lagrange multipliers are used to enforce boundary conditions, e.g. [5, 9], or interface coupling conditions e.g. [8, 4, 24]. In modeling reservoir flows [12], tissue perfusion [11, 13, 22] or soil-root interaction [21] resolving the interface as a manifold of codimension 1 can be prohibitively expensive. In this case it is convenient to represent the three-dimensional structures as curves and the model reduction gives rise to multiscale systems with a dimensionality gap 2.

Crucial for the FEM discretization of the multiscale models is the assembly of coupling terms, in particular, integration over the coupling manifold. There exists a number of open source FEM libraries, e.g. [7, 1, 19, 16], which expose this (low-level) functionality and as such can be used for implementation. However, for rapid

---

Miroslav Kuchta  
Simula Research Laboratory, P.O. Box 134, 1325 Lysaker, Norway, e-mail: miroslav@simula.no

prototyping, it is advantageous if the new models are described in a more abstract way which is closer to the mathematical definition of the problem.

FEniCS is a popular open source FEM framework which employs a compiler to generate low level (C++) assembly code from the high-level symbolic representation of the variational forms in the UFL language embedded in Python, see [25]. Here the code generation pipeline provides convenience for the user. At the same time, implementing new features is complicated by the fact that interaction with all the components of the pipeline is required. As a result, support for multiscale models has only recently been added to the core of the library [14] and is currently limited to problems with dimensionality gap 0 and 1. Moreover, in case of the trace constrained systems the coupling manifold needs to be triangulated in terms of facets of the bulk discretization. We remark that similar functionality for multiscale systems is offered by the FEniCS based library [2].

Here we present a simple algorithm<sup>1</sup> which extends FEniCS to support a more general class of multiscale systems by transforming symbolic variational forms in UFL language into a domain specific language [26] which represents (actions of) discrete linear operators. As this representation targets solutions by iterative methods preconditioning strategies shall also be discussed. Our work is structured as follows. Section 2 details the algorithm. Numerical examples spanning dimensionality gap 0, 1 and 2 are presented in §3 and §4 respectively.

## 2 Multiscale assembler

In the following  $(\cdot, \cdot)_\Omega$  denotes the  $L^2$  inner product over a bounded domain  $\Omega \subset \mathbb{R}^d$ ,  $d = 1, 2, 3$ . The duality pairing between the Hilbert space  $V$  and its dual space  $V'$  is denoted by  $(\cdot, \cdot)$ . Given basis of a discrete finite element space  $V_h$ , the matrix representation of operator  $A$  is  $A_h$ . Adjoints of  $A$  and  $A_h$  are denoted as  $A'$  and  $A'_h$  respectively.

Our representation of multiscale systems builds on two observations, which shall be presented using the Babuška problem [5]. Let  $\Gamma = \partial\Omega$  and  $V = H^1(\Omega)$ ,  $Q = H^{-1/2}(\Gamma)$ ,  $W = V \times Q$ . Then for every  $L \in W'$  there exists a unique solution  $w = (u, p) \in W$  satisfying  $\mathcal{A}w = L$  where

$$\mathcal{A} = \begin{pmatrix} A & B' \\ B & 0 \end{pmatrix} \quad \text{and} \quad \begin{aligned} (Au, v) &= (\nabla u, \nabla v)_\Omega + (u, v)_\Omega \quad v \in V, \\ (Bu, q) &= (Tu, q)_\Gamma \quad q \in Q. \end{aligned} \quad (1)$$

Here  $T : H^1(\Omega) \rightarrow H^{1/2}(\Gamma)$  is the trace operator such that  $Tu = u|_\Gamma$ ,  $u \in C(\overline{\Omega})$ . We remark that (1) is the weak form of  $-\Delta u + Iu = f$  in  $\Omega$  with  $u = g$  on  $\partial\Omega$  enforced by the Lagrange multiplier  $p$ .

---

<sup>1</sup> Implementation can be found in the Python module FEniCS<sub>ii</sub> [https://github.com/MiroK/fenics\\_ii](https://github.com/MiroK/fenics_ii)

Given the structure of  $\mathcal{A}$  in (1) it is natural to represent the operator on a finite element space  $W_h$  as a block structured matrix (rather than a monolithic one). Moreover, observe that the *multiscale* operator  $B : V \rightarrow Q$  (operator  $A : V \rightarrow V'$  is *singlescale*) is a composition  $B = I \circ T$  where  $I : H^{1/2}(\Gamma) \rightarrow Q$  is a singlescale operator. Therefore, matrix representation of  $B$  is a matrix product  $B_h = I_h T_h$ . Assuming that the FEM library at hand can only assemble singlescale operators, e.g.  $I$  and  $A$ , the multiscale operators  $B_h$  and  $\mathcal{A}_h$  can be formed if representation of the trace operator is available. We remark that the block representation is advantageous for construction of preconditioners; for example the blocks can be easily shared between the system and the preconditioner, cf. [20, 26].

Based on the above observations the multiscale systems can be represented as block structured operators where the blocks are not necessarily matrices. `Cbc.block` [26] defines a language for matrix expressions using the lazy evaluation pattern. In particular, `block matrix(block_mat)` and `matrix product(*)` are built-in operators. We remark that the operators are not formed explicitly, however, they can be evaluated if e.g. action in a matrix-vector product in a Krylov solver is needed. Using  $B$  from (1) as an example we thus aim to build an interpreter which translates UFL representation of  $(Tu, q)_\Gamma$  into a `cbc.block` representation  $I_h * T_h$ . We remark that  $T_h$  is here assumed to be a mapping between primal representations, cf. [27].

The core of the multiscale interpreter is the algorithm (Figure 1) translating between the two symbolic representations. Observe that in `multi_assemble` different *reduced* assemblers are recursively called on the transformed UFL form with the singlescale form being the base case. An example of a reduced assembler is the `trace_assemble` function which, having found *trace-reduced* argument (ln. 12) in form  $a$ , e.g.  $a(u, q) = (Bu, q) = (Tu, q)_\Gamma$ ,  $u \in V_h$ ,  $q \in Q_h$  builds a finite element *trace space*  $\tilde{V}_h = \tilde{V}_h(\Gamma)$  (ln. 14), an algebraic representation of the operator  $T : V_h \rightarrow \tilde{V}_h$  (ln. 15) and delegates assembly of the transformed form  $I(\tilde{u}, q) = (\tilde{u}, q)_\Gamma$ ,  $\tilde{u} \in \tilde{V}_h$ ,  $q \in Q_h$  (ln. 19) to `multi_assemble` (ln. 20). As  $I$  is singlescale the native FEniCS `assemble` function can be used to form the matrix  $I_h$  and the symbolic matrix-matrix product representation can be formed (ln. 20). The translation can thus be summarized as  $(Tu, q)_\Gamma \rightarrow (\tilde{u}, q)_\Gamma * T_h \rightarrow I_h * T_h$ .

Algorithm 1 can be easily extended to different multiscale couplings by adding a dedicated assembler. In particular, given  $\Omega \subset \mathbb{R}^3$  and  $\gamma$  a curve contained in  $\Omega$ , the *3d-1d* coupled problems [13, 12] require operators  $T, \Pi$  such that for  $u = C(\Omega)$ ,  $Tu = u|_\gamma$  and

$$(\Pi u)(x) = |C_R(x)|^{-1} \int_{C_R(x)} u(y) dy. \quad (2)$$

Here  $C_R(x)$  is a circle of radius  $R$  in a plane  $\{y \in \mathbb{R}^3, (y - x) \cdot \frac{dy}{ds}(x) = 0\}$  defined by the tangent vector of  $\gamma$  at  $x$ . We remark that assembling *3d-1d* constrained operators follows closely Algorithm 2, with the non-trivial difference being the representation of  $\Pi$ . We remark that in assembly of  $\Pi$  or  $T$  we do not require that  $\gamma$  is discretized in terms of edges of the mesh of  $\Omega$ . In fact, the two meshes can be independent. This is also the case for  $d-(d-1)$  trace. Let us also note that the restriction operator  $Ru = u|_\omega$ , where  $\omega \subseteq \Omega \subset \mathbb{R}^d$  can be implemented similar to the trace operator.

Algorithm 1: multi_assemble	Algorithm 2: trace_assemble
<pre> <b>Data:</b> a::UFL.Form or list of UFL.Form <b>Result:</b> cbc.block matrix expression 1 <b>begin</b>   // Single form 2   <b>if</b> a is UFL.Form <b>then</b>     // Attempt to reduce 3     <b>for</b> assembler <math>\in</math> assemblers <b>do</b> 4       tensor = assemble(a) 5       <b>if</b> tensor is not None <b>then</b> 6         <math>\lfloor</math> <b>return</b> tensor     // Singlescale operator 7     <b>return</b> FEniCS.assemble(a)   // Functional 8   <b>if</b> is_number(form) <b>then</b> 9     <math>\lfloor</math> <b>return</b> form 10  shape <math>\leftarrow</math> sizes(form)   // Assemble blocks 11  blocks <math>\leftarrow</math> map(multi_assemble, form)   // List/List of operators 12  tensor <math>\leftarrow</math> reshape(blocks, shape)   // Reshape for cbc.block   // Form had test functions only 13  <b>if</b> is_vector(tensor) <b>then</b> 14    <math>\lfloor</math> <b>return</b> block.block_vec(tensor)   // Bilinear form 15  <b>return</b> block.block_mat(tensor) </pre>	<pre> <b>Data:</b> a::UFL.Form <b>Result:</b> cbc.block matrix expression 1 <b>begin</b> 2  trace_integrals <math>\leftarrow</math> get_trace_integrals(a) 3  all_integrals <math>\leftarrow</math> integrals(form) 4  <b>if</b> not trace_integrals <b>then</b> 5    <math>\lfloor</math> <b>return</b> None   // Form is sum of integrals... 6  cs <math>\leftarrow</math> [] 7  <b>for</b> i <math>\in</math> all_integrals <b>do</b> 8    <b>if</b> i <math>\notin</math> trace_integrals <b>then</b> 9      cs += [multi_assemble(Form([i]))] 10   <b>continue</b> 11  integrnd <math>\leftarrow</math> integrand(i) 12  u, <math>\leftarrow</math> trace_terminals(intgrnd) 13  V<sub>h</sub> <math>\leftarrow</math> function_space(u) 14  <math>\tilde{V}_h</math> <math>\leftarrow</math> trace_space(V<sub>h</sub>, u) 15  T<sub>h</sub> <math>\leftarrow</math> trace_matrix(V<sub>h</sub>, <math>\tilde{V}_h</math>) 16  <b>if</b> is_trial_function(u) <b>then</b> 17    <math>\bar{u}</math> <math>\leftarrow</math> TrialFunction(<math>\tilde{V}_h</math>) 18    ii <math>\leftarrow</math> replace(intgrnd, u, <math>\bar{u}</math>) 19    I = Form([reconstruct(i, ii)]) 20    B<sub>h</sub> <math>\leftarrow</math> multi_assemble(I)*T 21    cs += [B<sub>h</sub>]   // Handle test/function   // ...cbc.block sum of operators 22  <b>return</b> reduce(+, cs) </pre>

Fig. 1: Translation of UFL representation of multiscale variational form into cbc.block matrix expression. Several passes by different scale assemblers might be needed to reduce the form into base case singlescale which can be assembled as matrix or vector by FEniCS. Handling of test function and function type terminals is omitted for brevity.

Finally, observe that the Algorithm 1 is not limited to forms where the arguments are *reduced* to the coupling manifold. Indeed, [12, 18] utilize *extension* from  $\gamma$  to  $\Omega$  by a constant or as Green function of a line source respectively. Such couplings can be readily handled if realization of the discrete *extension* operator is available.

We conclude the discussion by listing the limitations of our current implementation. Unlike in [14, 2] the MPI-parallelism is missing<sup>2</sup> as is the support for nonlinear forms. Moreover, the reduction operators cannot be nested and can only be applied to terminal expressions in UFL, e.g.  $T(u + v)$  cannot be interpreted. In addition, point constraints are not supported. With the exception of parallelism the limitations should be addressed by future versions.

<sup>2</sup> The serial performance of our pure Python implementation is cca. 2x slower than the native FEniCS implementation [14]. More precisely, assembling (1) on  $\Omega = [0, 1]^2$  discretized by  $2 \cdot 1024^2$  triangles and continuous linear Lagrange elements (the system matrix size is approx  $10^6$ , however, it is *not* explicitly formed here) takes 3.86s (to be compared with 1.79s). Most of the time is spent building  $T_h$ . The trace matrix is reused by the interpreter to evaluate both  $B_h$  and  $B'_h$ .

In the following we showcase the multiscale interpreter by considering coupled problems with dimensionality gap 0, 1 and 2. We begin by a trace constrained  $2d-1d$  Darcy-Stokes system.

### 3 Trace constrained systems

Let  $\Omega_1, \Omega_2 \subset \mathbb{R}^2$  be such that  $\Gamma = \partial\Omega_1 \cap \partial\Omega_2$  and  $|\Gamma| \neq 0$ . Further let  $\partial\Omega_i = \Gamma \cup \Gamma_i^D \cup \Gamma_i^N$  where  $|\Gamma_i^k| \neq 0, i = 1, 2, k = N, D$  and  $\Gamma \cap \Gamma_i^N = \emptyset$ , cf. Figure 2. We then wish to solve the Darcy-Stokes problem (with unit parameters)

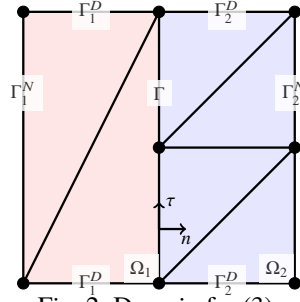


Fig. 2: Domain for (3).

$$-\nabla \cdot \sigma = f_1 \quad \text{in } \Omega_1, \quad (3a)$$

$$\nabla \cdot u_1 = 0 \quad \text{in } \Omega_1, \quad (3b)$$

$$u_2 + \nabla p_2 = 0 \quad \text{in } \Omega_2, \quad (3c)$$

$$\nabla \cdot u_2 = f_2 \quad \text{in } \Omega_2, \quad (3d)$$

$$u_1 \cdot n - u_2 \cdot n = 0 \quad \text{on } \Gamma, \quad (3e)$$

$$n \cdot \sigma \cdot n + p_2 = 0 \quad \text{on } \Gamma, \quad (3f)$$

$$-n \cdot \sigma \cdot \tau - u_1 \cdot \tau = 0 \quad \text{on } \Gamma. \quad (3g)$$

Here  $\sigma(u_1, p_1) = D(u_1) - p_1 I$  with  $D(u) = \frac{1}{2}((\nabla u) + (\nabla u)')$ . The unknowns  $u_1, p_1$  and  $u_2, p_2$  are respectively the Stokes and Darcy velocity and pressure. The system is closed by prescribing Dirichlet conditions on  $\Gamma_i^D$  and Neumann conditions on  $\Gamma_i^N$ .

Let  $T_n, T_t$  be the normal and tangential trace operators on  $\Gamma$ . We shall consider variational formulations of (3) induced by a pair of operators

$$\mathcal{A}_p = \left( \begin{array}{c|c} -\nabla \cdot D + T_t' T_t & -\nabla \\ \hline \text{div} & I \quad -\nabla \\ \hline -T_n & \text{div} \\ \hline & -\Delta \end{array} \right), \quad \mathcal{A}_m = \left( \begin{array}{c|c|c} -\nabla \cdot D + T_t' T_t & -\nabla & T_n' \\ \hline \text{div} & I \quad -\nabla & -T_n' \\ \hline & \text{div} & \\ \hline T_n & -T_n & \end{array} \right). \quad (4)$$

Using the (mixed) operator  $\mathcal{A}_m$  problem (3) is solved for both  $u_2, p_2$  and an additional unknown, the Lagrange multiplier, which enforces mass conservation  $u_1 \cdot n - u_2 \cdot n = 0$  on  $\Gamma$ . In the (primal) operator  $\mathcal{A}_p$  the condition appears naturally. Observe that the operator is non-symmetric.

Well-posedness of the primal and mixed formulations as well the corresponding solution strategies have been studied in a number of works, e.g [15] and [24, 17]. Here we compare the formulations and discuss monolithic solvers which utilize block diagonal preconditioners

$$\begin{aligned} \mathcal{B}_p &= \text{diag} \left( -\nabla \cdot D + T'_i T_i, I, -I \right)^{-1}, \\ \mathcal{B}_m &= \text{diag} \left( -\nabla \cdot D + T'_i T_i, I, I - \nabla \text{div}, I, (-\Delta + I)^{1/2} \right)^{-1}. \end{aligned} \quad (5)$$

Here the preconditioner  $\mathcal{B}_p$  has been proposed by [10], while  $\mathcal{B}_m$  follows from the analysis [17] by operator preconditioning technique [27]. More precisely,  $\mathcal{B}_m$  is a Riesz map with respect to the inner product of the space in which [17] prove well-posedness of  $\mathcal{A}_m$ , i.e.  $H^1_{0,\Gamma^p}(\Omega_1) \times L^2(\Omega_1) \times H_{0,\Gamma^p}(\text{div}, \Omega_2) \times L^2(\Omega_2) \times H^{1/2}(\Gamma)$ . We remark that all the blocks of the preconditioners can be realized by efficient and order optimal multilevel methods. In particular, we shall use further the multigrid realization of the fractional Laplace preconditioner [6].

In order to check mesh independence of the preconditioners let us consider the geometry from Figure 2 and let  $\Omega_1 = [0, 0.5] \times [0, 1]$ ,  $\Omega_2 = [0.5, 1] \times [0, 1]$ . In both  $\mathcal{A}_m$ ,  $\mathcal{A}_p$  the triangulations of the domains shall be *independent*<sup>3</sup>, cf. Figure 2, with the mesh of  $\Gamma$  defined in terms of facets of  $\Omega_2$ . Finally, the finite element approximation of  $\mathcal{A}_p$  shall be constructed using  $P_2$ - $P_1$ - $P_2$  elements<sup>4</sup> while  $P_2$ - $P_1$ - $RT_0$ - $P_0$ - $P_0$  is used for the mixed formulation  $\mathcal{A}_m$ .

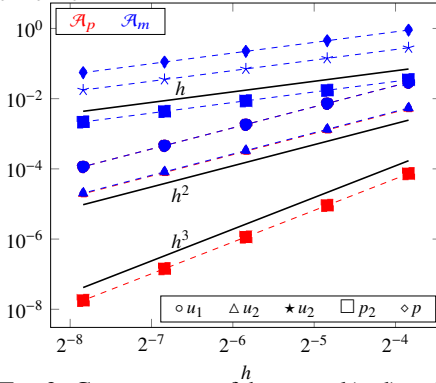


Fig. 3: Convergence of the primal (red) and mixed formulation of (3). The approximation error is computed in the norms of  $\mathcal{B}_p^{-1}$  and  $\mathcal{B}_m^{-1}$ .

Table 1: Number of iterations required for convergence of  $\text{GMRes}(\mathcal{A}_p)$  and  $\text{MinRes}(\mathcal{A}_m)$  using preconditioners (5), see also implementation in Figure 4. Multigrid preconditioner for  $H^{1/2}$  leads to slightly increased number of iterations compared to eigenvalue realization [23].

$h$	$\mathcal{B}_p \mathcal{A}_p$	$\mathcal{B}_p^{\text{EIG}} \mathcal{A}_p$	$\mathcal{B}_p^{\text{MG}} \mathcal{A}_p$
$2^{-3}$	48	53	59
$2^{-4}$	48	51	59
$2^{-5}$	47	50	63
$2^{-6}$	47	49	65
$2^{-7}$	46	49	65

Results of the numerical experiment are summarized in Table 1. It can be seen that the preconditioners (5) are robust with respect to the discretization. Further, Figure 3 shows that both formulations lead to expected order of convergence in all the unknowns. The approximation of Stokes variables is practically identical. We remark that  $p_2$  convergence in  $\mathcal{A}_p$  is reported in the  $L^2$  norm for the sake of

<sup>3</sup> Details of experimental setup. We discretize  $\Omega_i$  uniformly by first dividing the domains into  $n \times m$  rectangles and afterwards splitting each rectangle into two triangles. For  $\Omega_1$  we have  $m = n$ ,  $m = 2n$  for  $\Omega_2$  so that the trace meshes of the domains are different. Krylov solvers are started from random initial guess. Convergence tolerance for relative preconditioned residual norm of  $10^{-10}$  is used. Unless specified otherwise the preconditioner blocks use LU factorization.

<sup>4</sup> Finite element space of continuous Lagrange elements of order  $k$  is denoted by  $P_k$  while  $RT_0$  denotes the space of lowest order Raviart-Thomas elements.

```

def mixed_darcy_stokes_system(n):
    '''Coupled Stokes-Darcy'''
    # Omega1 [0, 0.5]x[0, 1] as nxn, Omega2 nx2n
    # W = [P2]^2 x P1 x R0 x P0 x P0
    W = [V1, Q1, V2, Q2, Q]

    u1, p1, u2, p2, p = map(TrialFunction, W)
    v1, q1, v2, q2, q = map(TestFunction, W)
    # Stokes traces
    Tu1, Tv1 = Trace(u1, gamma), Trace(v1, gamma)
    # Darcy traces
    Tu2, Tv2 = Trace(u2, gamma), Trace(v2, gamma)
    # Coupled integration
    dl = Measure('dx', domain=gamma)
    n, tau = Constant((1, 0)), Constant((0, 1))

    a = block_form(W, 2)
    # Stokes
    a.add(inner(sym(grad((u1))), sym(grad(v1))))*dx +
          inner(dot(Tu1, tau), dot(Tv1, tau))*dl
          - inner(q1, div(u1))*dx
          - inner(p1, div(v1))*dx)
    # Darcy
    a.add(inner(u2, v2)*dx - inner(p2, div(v2))*dx -
          inner(q2, div(u2))*dx)
    # Coupling
    a.add(
        inner(p, dot(Tv1, n))*dl - inner(p, dot(Tv2, n))*dl
        - inner(q, dot(Tu1, n))*dl - inner(q, dot(Tu2, n))*dl
    )
    # Define rhs + boundary conditions
    A, b = map(ii_assemble, (a, L))

    return A, b, W

def mixed_darcy_stokes_preconditioner(W, AA):
    '''H1 x L2 x Hdiv x L2 x H^{0.5}'''
    V1, Q1, V2, Q2, Q = W
    # Stokes velocity
    Vr = LU(AA[0][0])
    # Stokes pressure
    p, q = TrialFunction(Q1), TestFunction(Q1)
    Q1r = LU(assemble(inner(p, q)*dx)) # Or AMG

    # Darcy velocity
    mesh2 = V2.mesh()
    bcs = DirichletBC(V2,
                      Constant((0, 0)),
                      'near(x[1]*(1-x[1]), 0)')

    u, v = TrialFunction(V2), TestFunction(V2)
    a = inner(u, v)*dx + inner(div(u), div(v))*dx
    L = inner(Constant((0, 0)), v)*dx
    # Need symmetric assembly
    Hdiv_inner, _ = assemble_system(a, L, bcs)
    V2r = LU(Hdiv_inner) # or HypreAMS

    # Darcy pressure
    p, q = TrialFunction(Q2), TestFunction(Q2)
    Q2r = LU(assemble(inner(p, q)*dx)) # or AMG
    # Multiplier H^s norm by Eigvp ...
    # Qr = HsNorm(Q, s=0.5, bcs=False)**-1
    # ... or multigrid
    Qr = HsNormMG(Q, s=0.5, bdry=None, s=0.5,
                  mg_params={'nlevels': 3,
                             'eta': 0.4,
                             'macro_size': 1'})

    return block_diag_mat([V1r, Q1r, V2r, Q2r, Qr])

```

Fig. 4: Implementation of mixed Darcy-Stokes problem. (Left) Definition of the problem operator. (Right) Complete implementation of  $\mathcal{B}_m$  preconditioner using either eigenvalue [23] or multigrid [6] realization of the fractional Laplacian.

comparison with the mixed formulation. Implementation of  $\mathcal{A}_m$  and preconditioner  $\mathcal{B}_m$  can be found in Figure 4.

## 4 More general multiscale systems

To show flexibility of the interpreter we finally consider a simple prototypical  $3d-1d$  coupled problem and an extended Darcy-Stokes problem with  $2d-2d-1d$  coupling. We will present both problems before discussing the results.

Let  $\Omega \subset \mathbb{R}^3$  be a bounded domain and let  $\gamma$  be a curve embedded in  $\Omega$ . Assuming  $\gamma$  is a representation of the vasculature (e.g. as center lines) parameterized by arc length coordinate  $s$  a model of tissue *perfusion* by [13] is given as

$$\begin{aligned}
 -\nabla \cdot (k \nabla u) + \beta(\Pi u - p) \delta_\gamma &= 0 & \text{in } \Omega, \\
 -\frac{d}{ds} \left( \hat{k} \frac{d}{ds} p \right) - \beta(\Pi u - p) &= 0 & \text{on } \gamma.
 \end{aligned} \tag{6}$$

Here  $k, \hat{k}$  are the conductivities of the tissue and the vasculature, while  $\beta$  is the permeability. Observe that the exchange term is localized in  $\Omega$  by the Dirac function  $\delta_\Gamma$ .

Let next  $\Omega_i \subset \mathbb{R}^d$ ,  $d = 2, 3$ ,  $i = 1, 2$  be the fluid domain and a porous domain which share a common interface  $\Gamma$ . A model for *transport* of a scalar  $\phi$  in such a medium  $\Omega = \Omega_1 \cup \Omega_2$  was recently analyzed by [3]. Here we shall consider a simplified, linearized version of the system

$$\begin{aligned} -\nabla \cdot \sigma + g\phi &= f_1 && \text{in } \Omega_1, \\ \nabla \cdot u_1 &= 0 && \text{in } \Omega_1, \\ u_2 + \nabla p_2 + g\phi &= 0 && \text{in } \Omega_2, \\ \nabla \cdot u_2 &= f_2 && \text{in } \Omega_2, \\ -\Delta\phi + \nabla \cdot fu_1 + \nabla \cdot fu_2 &= 0 && \text{in } \Omega, \end{aligned} \quad (7)$$

where  $g$  and  $f$  are given vector and scalar fields on  $\Omega$ . We remark that (7) is considered with the interface conditions (3e)-(3g).

Compared to Babuška problem (1) or Darcy-Stokes problem (4) systems (7) and (6) introduce new multiscale couplings

$$\mathcal{A}_p = \begin{pmatrix} -k\Delta + T'\Pi & \beta T' \\ -\beta\Pi & -\hat{k}\Delta + \beta I \end{pmatrix}, \quad \mathcal{A}_t = \left( \begin{array}{c|c|c|c} -\nabla \cdot D + T'_t T_t & -\nabla & T'_n & R'_1 \\ \text{div} & & & \\ \hline & I & -\nabla & -T'_n \\ & \text{div} & & R'_2 \\ \hline T_n & -T_n & & \\ \hline \text{div} \circ R_1 & \text{div} \circ R_2 & & -\Delta \end{array} \right). \quad (8)$$

Indeed, in the perfusion operator  $\mathcal{A}_p$  the test functions in the bulk are reduced to  $\gamma$  by a  $3d-1d$  trace operator while  $\Pi$  in (2) is used for the trial functions. The transport operator  $\mathcal{A}_t$  then uses restriction operators  $R_i\phi = \phi|_{\Omega_i}$ ,  $i = 1, 2$  for  $\phi \in C(\Omega)$ . We remark that differently weighted Sobolev spaces are required in order for the  $3d-1d$  reduction operators to be well defined, see [13]. In particular, the trace operator requires higher than  $H^1$  regularity.

We test the abilities of the assembler by considering FEM discretization of (6) in terms of  $P_1$ - $P_1$  elements while (7) shall be discretized by  $P_2$ - $P_1$ - $RT_0$ - $P_0$ - $P_0$ - $P_2$ . Here the setup for (6) mirrors §3. However, to simplify the restriction the meshes for  $\Omega_1$  and  $\Omega_2$  are not independent. Instead, they are defined using the triangulation of  $\Omega$ . The perfusion problem is then setup on a uniform discretization of  $[0, 1]^3$  with  $\gamma$  a straight line which, in general, is not aligned with the edges of the mesh of  $\Omega$ .

Figure 5 shows the error convergence of the two approximations. For (7) the error with respect to the manufactured solution is measured and the expected rates can be observed. In perfusion problem the relative norm of the refined solution decreases linearly.

## References

1. MFEM: Modular finite element methods library. [mfem.org](http://mfem.org). DOI 10.11578/dc.20171025.1248
2. multiphenics - easy prototyping of multiphysics problems in FEniCS. <https://mathlab.sissa.it/multiphenics>. Accessed: 2019-12-16



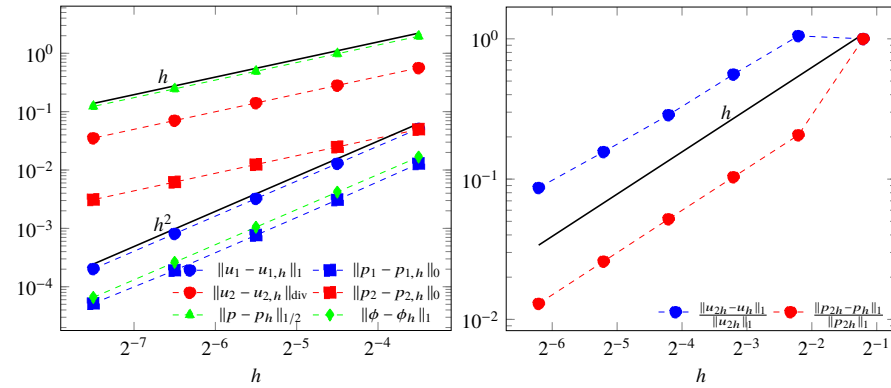


Fig. 5: Convergence of the FEM approximation of the  $2d$ - $2d$ - $1d$  coupled problem (7) and a  $3d$ - $1d$  problem (6).

3. Alvarez, M., Gatica, G.N., Ruz-Baier, R.: A mixed-primal finite element method for the coupling of Brinkman-Darcy flow and nonlinear transport. *IMA Journal of Numerical Analysis* (2019)
4. Ambartsumyan, I., Khattatov, E., Yotov, I., Zunino, P.: A Lagrange multiplier method for a Stokes–Biot fluid–poroelastic structure interaction model. *Numerische Mathematik* **140**(2), 513–553 (2018)
5. Babuška, I.: The finite element method with Lagrangian multipliers. *Numerische Mathematik* **20**(3), 179–192 (1973)
6. Bærland, T., Kuchta, M., Mardal, K.A.: Multigrid methods for discrete fractional Sobolev spaces. *SIAM Journal on Scientific Computing* **41**(2), A948–A972 (2019)
7. Bangerth, W., Hartmann, R., Kanschat, G.: deal.II – a general purpose object oriented finite element library. *ACM Trans. Math. Softw.* **33**(4), 24/1–24/27 (2007)
8. Bernardi, C., Maday, Y., Patera, A.T.: Domain decomposition by the mortar element method. In: *Asymptotic and numerical methods for partial differential equations with critical parameters*, pp. 269–286. Springer (1993)
9. Bertoluzza, S., Chabannes, V., Prud’Homme, C., Szopos, M.: Boundary conditions involving pressure for the Stokes problem and applications in computational hemodynamics. *Computer Methods in Applied Mechanics and Engineering* **322**, 58–80 (2017)
10. Cai, M., Mu, M., Xu, J.: Preconditioning techniques for a mixed Stokes/Darcy model in porous media applications. *Journal of computational and applied mathematics* **233**(2), 346–355 (2009)
11. Cattaneo, L., Zunino, P.: A computational model of drug delivery through microcirculation to compare different tumor treatments. *International journal for numerical methods in biomedical engineering* **30**(11), 1347–1371 (2014)
12. Cerroni, D., Laurino, F., Zunino, P.: Mathematical analysis, finite element approximation and numerical solvers for the interaction of 3d reservoirs with 1d wells. *GEM-International Journal on Geomathematics* **10**(1), 4 (2019)
13. D’Angelo, C., Quarteroni, A.: On the coupling of 1d and 3d diffusion-reaction equations: application to tissue perfusion problems. *Mathematical Models and Methods in Applied Sciences* **18**(08), 1481–1504 (2008)
14. Daversin-Catty, C., Richardson, C.N., Ellingsrud, A.J., Rognes, M.E.: Abstractions and automated algorithms for mixed domain finite element methods. *arXiv preprint arXiv:1911.01166* (2019)
15. Discacciati, M., Miglio, E., Quarteroni, A.: Mathematical and numerical models for coupling surface and groundwater flows. *Applied Numerical Mathematics* **43**(1-2), 57–74 (2002)

16. Fournié, M., Renon, N., Renard, Y., Ruiz, D.: CFD parallel simulation using GetFem++ and MUMPS. In: P. D'Ambra, M. Guarracino, D. Talia (eds.) Euro-Par 2010 - Parallel Processing, pp. 77–88. Springer Berlin Heidelberg, Berlin, Heidelberg (2010)
17. Galvis, J., Sarkis, M.: Non-matching mortar discretization analysis for the coupling Stokes-Darcy equations. *Electron. Trans. Numer. Anal.* **26**(20), 07 (2007)
18. Gjerde, I.G., Kumar, K., Nordbotten, J.M.: A singularity removal method for coupled 1d-3d flow models. *arXiv preprint arXiv:1812.03055* (2018)
19. Hecht, F.: New development in FreeFem++. *J. Numer. Math.* **20**(3-4), 251–265 (2012). URL <https://freefem.org/>
20. Kirby, R.C., Mitchell, L.: Solver composition across the PDE/linear algebra barrier. *SIAM Journal on Scientific Computing* **40**(1), C76–C98 (2018)
21. Koch, T., Heck, K., Schröder, N., Class, H., Helmig, R.: A new simulation framework for soil–root interaction, evaporation, root growth, and solute transport. *Vadose Zone Journal* **17**(1) (2018)
22. Koch, T., Schneider, M., Helmig, R., Jenny, P.: Modeling tissue perfusion in terms of 1d-3d embedded mixed-dimension coupled problems with distributed sources. *arXiv preprint arXiv:1905.03346* (2019)
23. Kuchta, M., Nordaas, M., Verschaeve, J.C., Mortensen, M., Mardal, K.A.: Preconditioners for saddle point systems with trace constraints coupling 2d and 1d domains. *SIAM Journal on Scientific Computing* **38**(6), B962–B987 (2016)
24. Layton, W.J., Schieweck, F., Yotov, I.: Coupling fluid flow with porous media flow. *SIAM Journal on Numerical Analysis* **40**(6), 2195–2218 (2002)
25. Logg, A., Mardal, K.A., Wells, G.: Automated solution of differential equations by the finite element method: The FEniCS book, vol. 84. Springer Science & Business Media (2012)
26. Mardal, K.A., Haga, J.B.: Block preconditioning of systems of PDEs, pp. 643–655. Springer Berlin Heidelberg, Berlin, Heidelberg (2012)
27. Mardal, K.A., Winther, R.: Preconditioning discretizations of systems of partial differential equations. *Numerical Linear Algebra with Applications* **18**(1), 1–40 (2011)